Electronic Supplementary Material (ESI) for Energy & Environmental Science.
This journal is © The Royal Society of Chemistry 2014

Electronic supplementary information

Transforming organic-rich amaranthus waste into nitrogen-doped carbon with superior performance of oxygen reduction reaction

Shuyan Gao,*[a] Keran Geng,[a] Haiying Liu,[b] Xianjun Wei,[a] Min Zhang,[c] Peng Wang*[c] and Jianji Wang*

[a] School of Chemistry and Chemical Engineering, Henan Normal University, Xinxiang 453007, China.

[b] School of Life and Life Sciences, Henan Normal University, Xinxiang 453007, China

[c] State Key Laboratory of Polymer Physics and Chemistry, Changchun Institute of Applied Chemistry, Chinese Academy of Sciences, Changchun 13002, China.

*Corresponding Author, Email: shuyangao@htu.cn; peng.wang@ciac.ac.cn; jwang@htu.cn

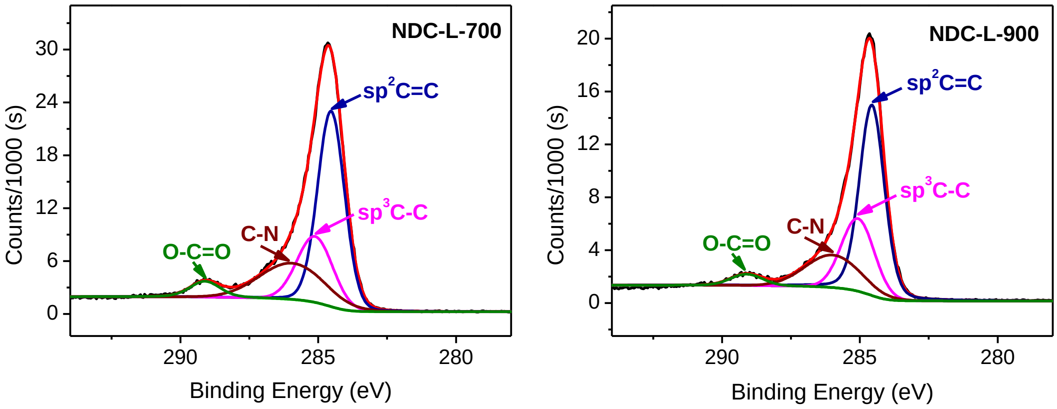

Fig. S1 C1s XPS spectra of NDC-L-700, NDC-L-900.

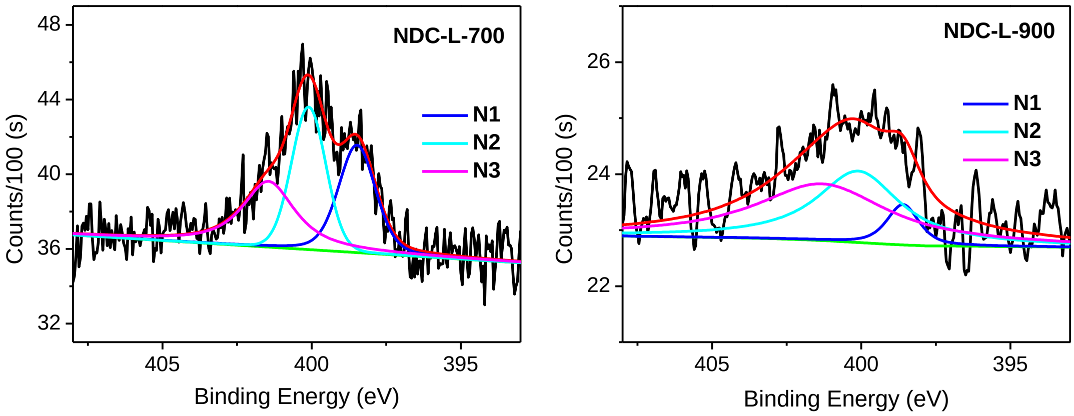

Fig. S2 High resolution N1s XPS scan of NDC-L-700, NDC-L-900.

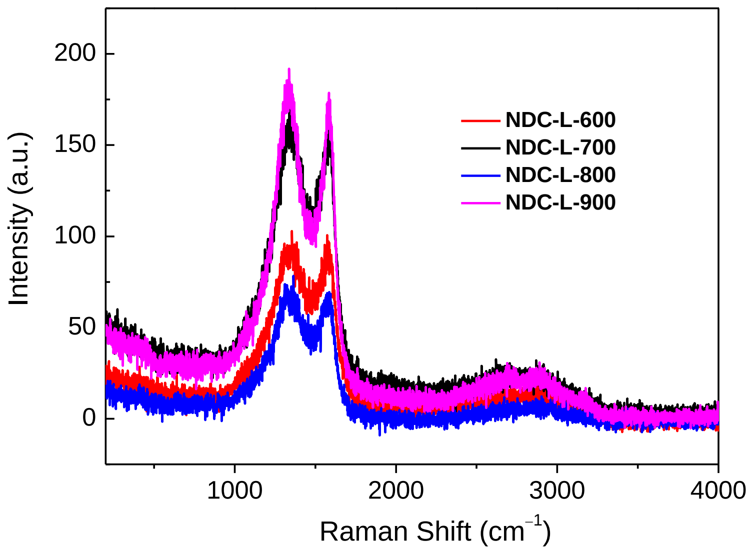

Fig. S3 Raman spectra of NDC-L-Y.

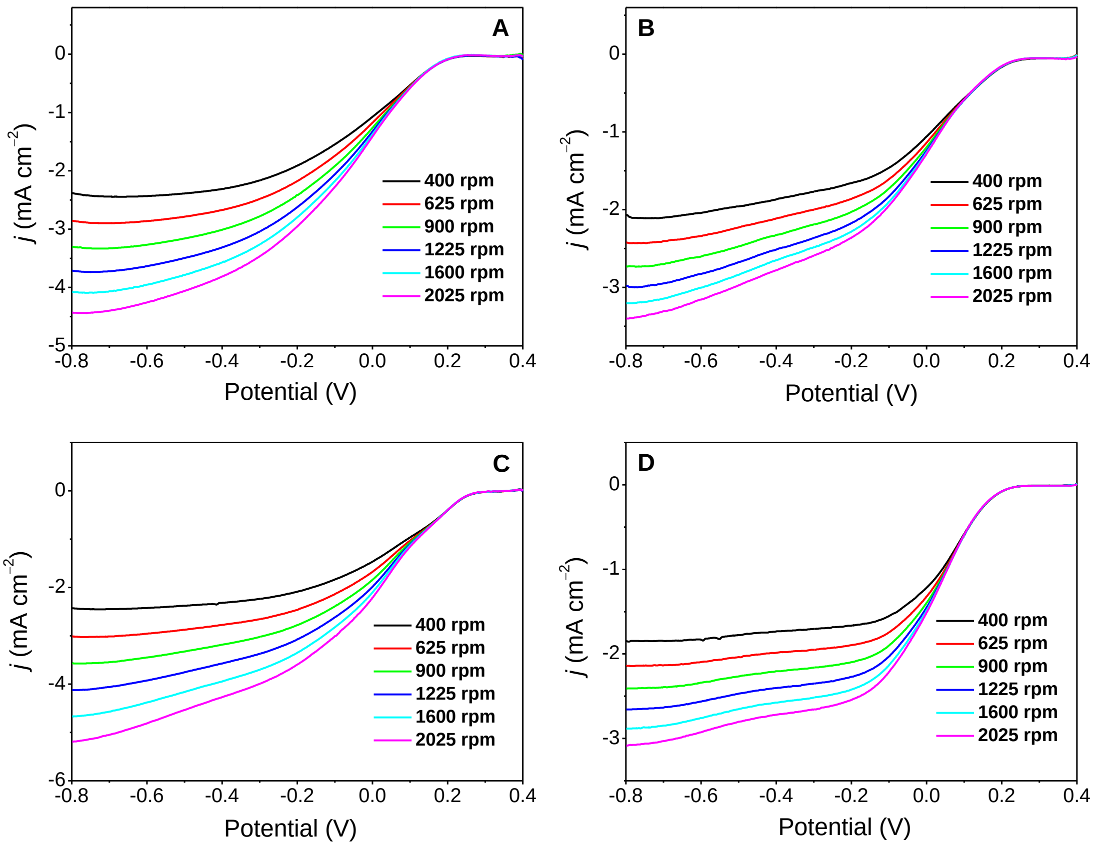

Fig. S4 A, B, C, D) RDE curves for NDC-L-600, NDC-L-700, NDC-L-800, NDC-L-900 in O_2-saturated 0.1 M KOH with a scan rate of 10 mV s^{-1} at different rotation speeds.

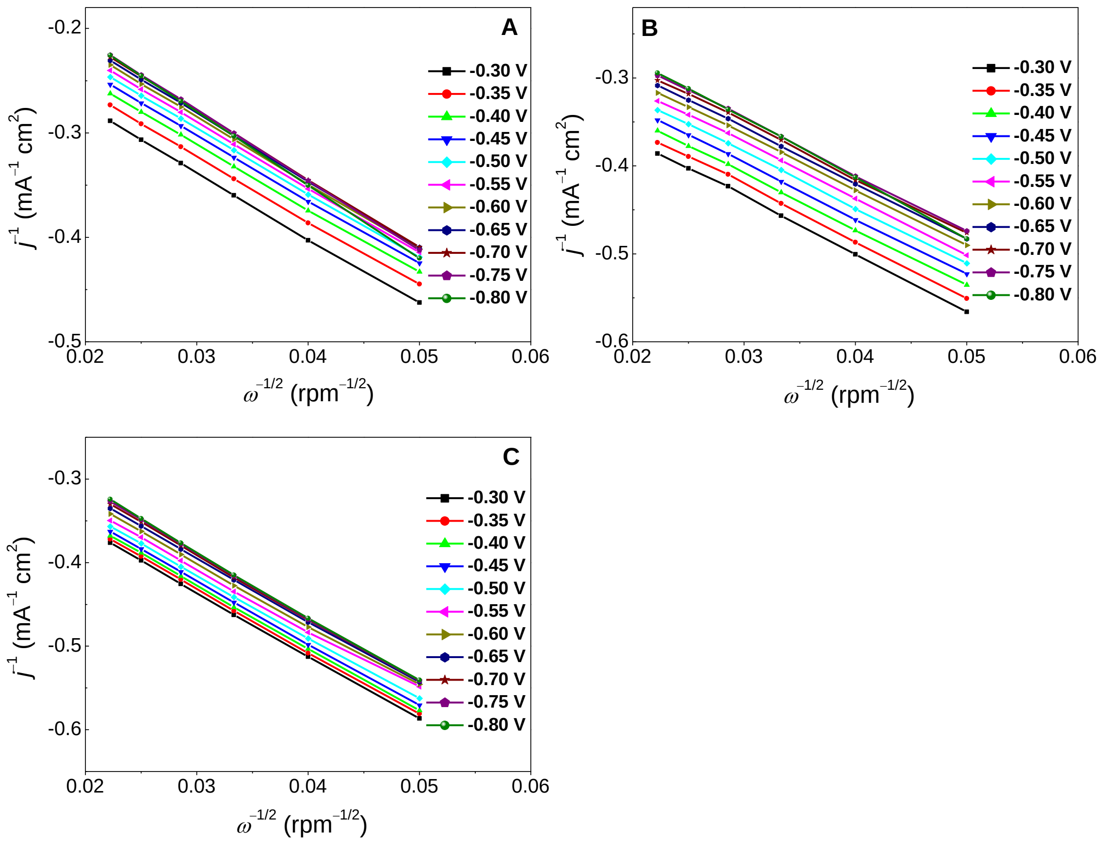

Fig. S5 A, B, C,) K-L plots for the ORR in O_2-saturated 0.1 M KOH solution for NDC-L-600, NDC-L-700, NDC-L-900.

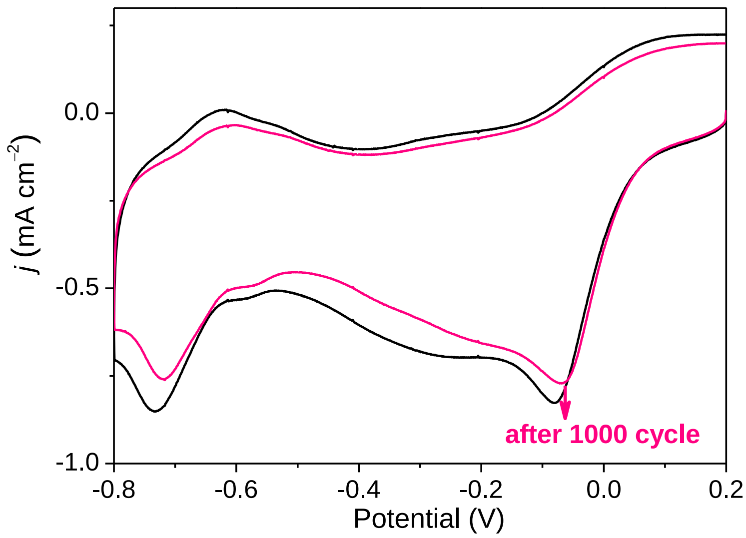

Fig. S6 Electrochemical stability of 20 wt% Pt/C as determined by continuous CV scanning in O_2-saturated 0.1 M KOH. Scan rate: 10 mV s^{-1}.

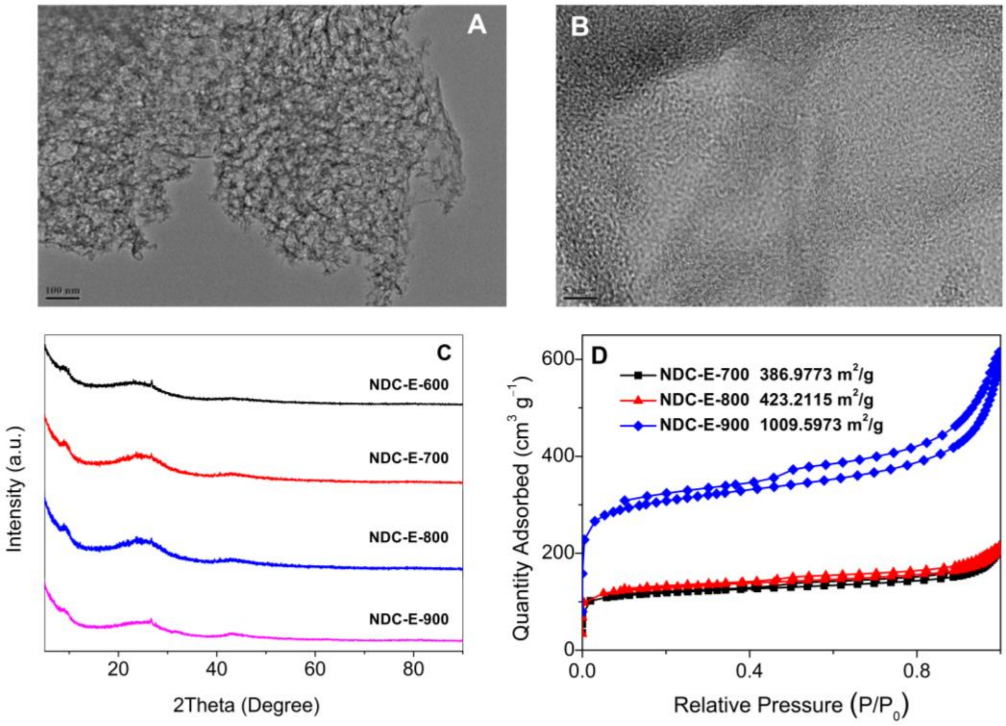

Fig. S7 A) TEM, B) HRTEM images of NDC-E-800. C, D) XRD patterns over the 2θ range of 5°−90° and N_2 adsorption–desorption isotherms of NDC-E-700, NDC-E-800, NDC-E-900.

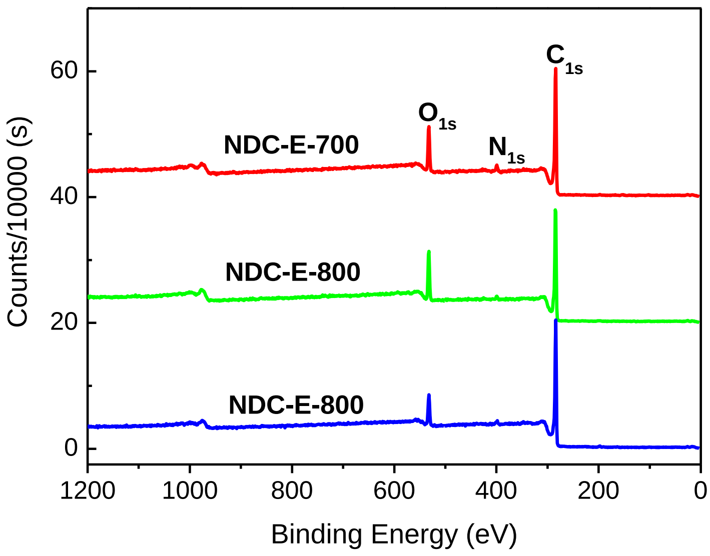

Fig. S8 Full-scan XPS of NDC-E-700, NDC-E-800, NDC-E-900.

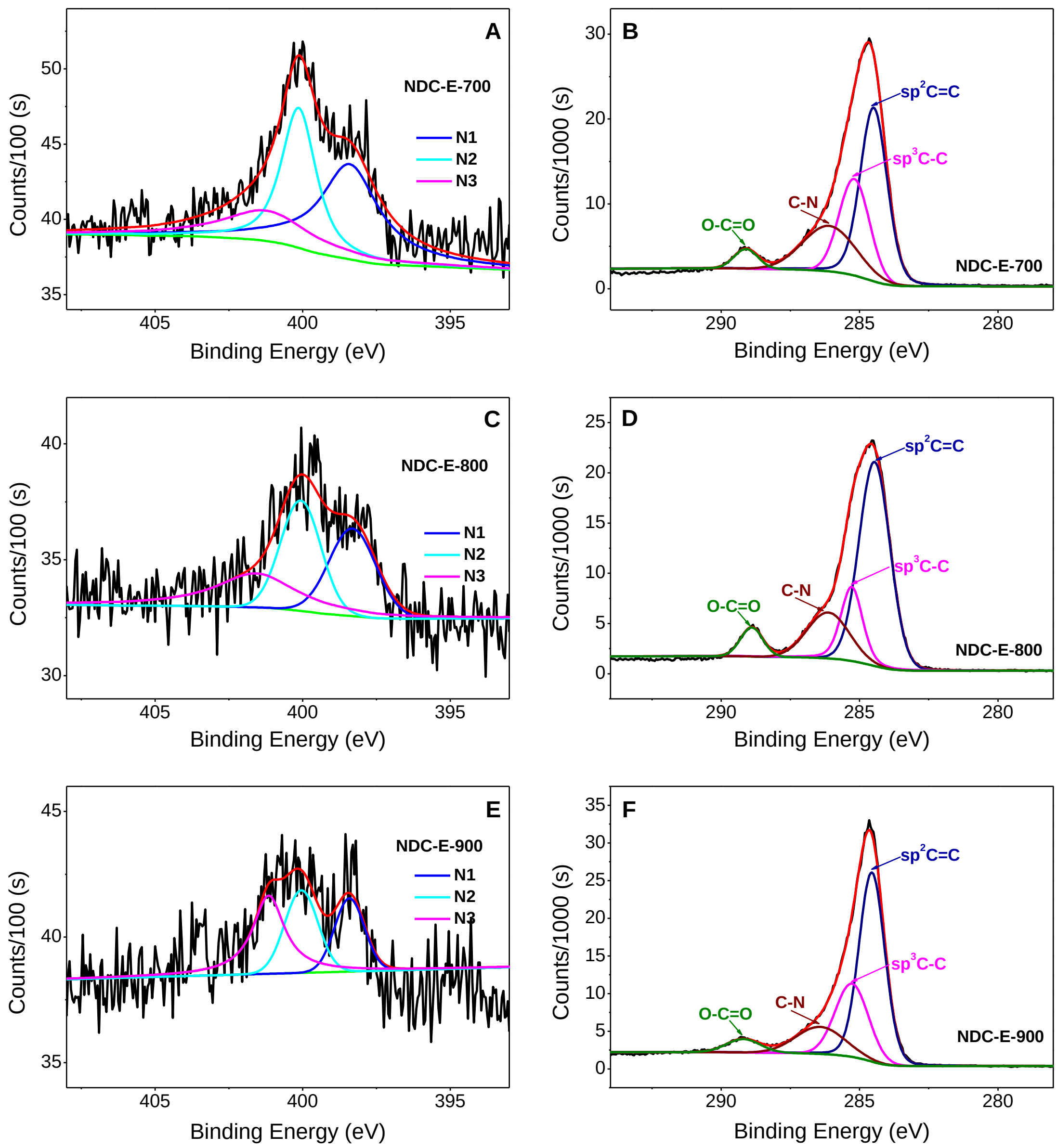

Fig. S9 High resolution N1s and C1s XPS scan of NDC-E-700, NDC-E-800, NDC-E-900.

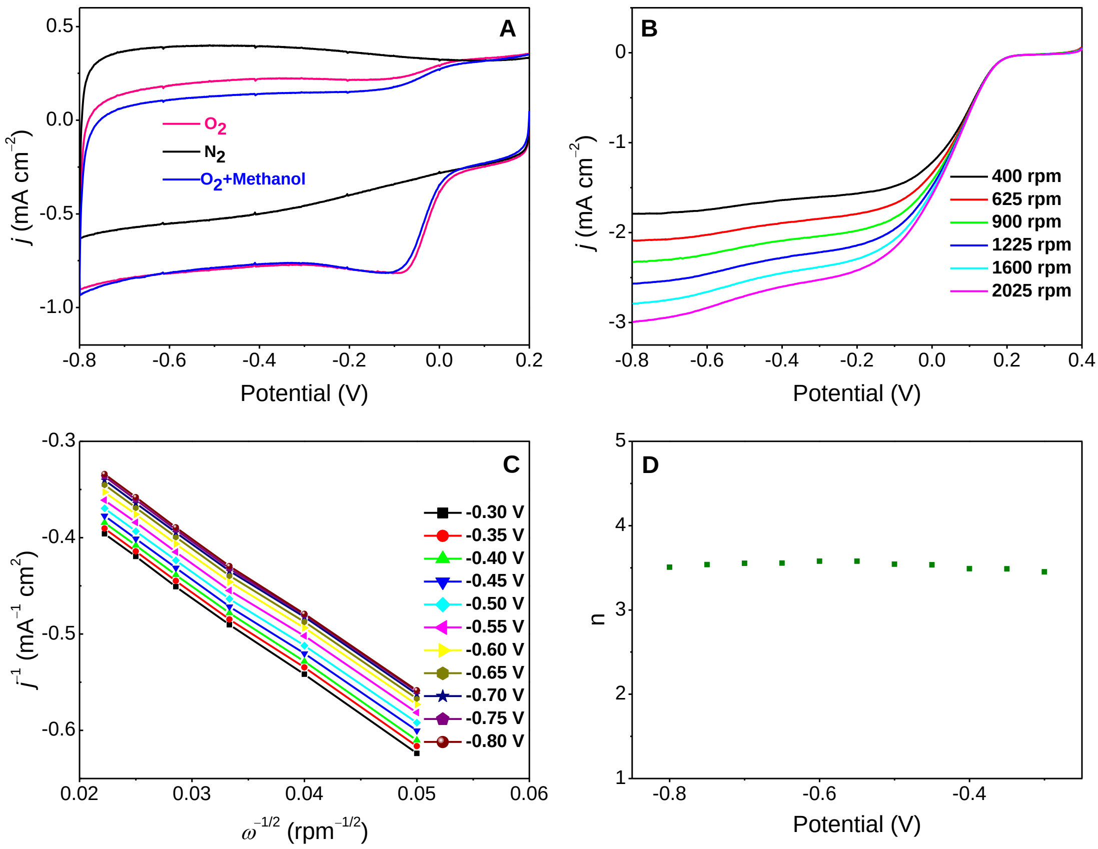

Fig. S10 A) CV curves of NDC-E-800 in N_2-saturated, O_2-saturated 0.1 M KOH solution, and O_2-saturated 0.1 M KOH with 10 vol% methanol at a scan rate of 10 mV s^{-1}. B) RDE curves for NDC-E-800 in O_2-saturated 0.1 M KOH with a scan rate of 10 mV s^{-1} at different rotation speeds. C) K–L plots for the ORR in O_2-saturated 0.1 M KOH solution for NDC-E-800. D) The electron number calculated from K–L plot.

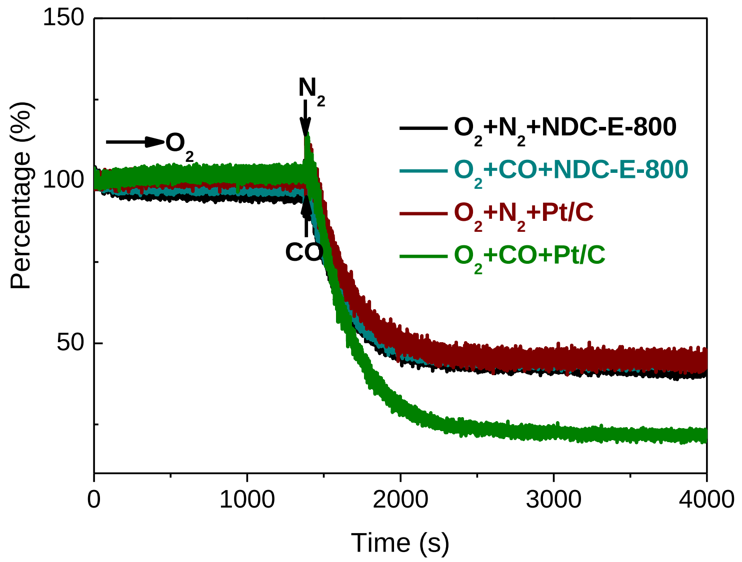

Fig. S11 The percentage of current density (*j*) vs. time chronoamperometric responses obtained at the NDC-E-800 and 20 wt% Pt/C electrodes at -0.30 V in O_2-saturated 0.1 M KOH. The arrow indicates the introduction of N_2 or CO into the electrolyte.

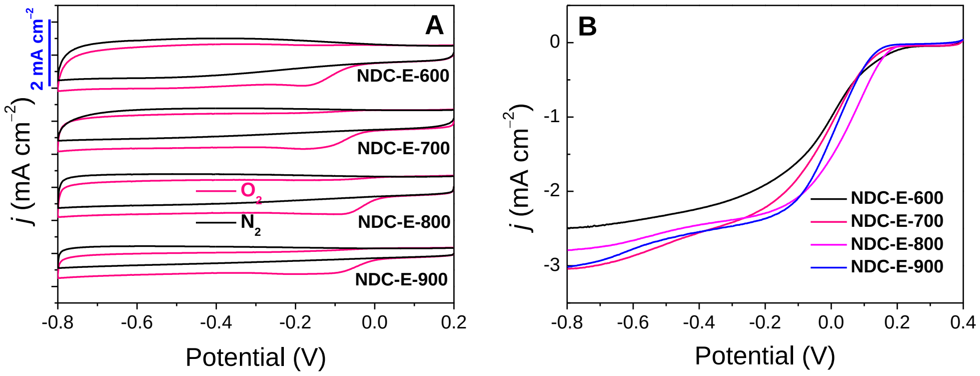

Fig. S12 A) CV curves of NDC-E-600, NDC-E-700, NDC-E-800, NDC-E-900 in N_2-saturated, O_2-saturated 0.1 M KOH solution at a scan rate of 10 mV s^{-1}. B) RDE curves for NDC-E-600, NDC-E-700, NDC-E-800, NDC-E-900 in O_2-saturated 0.1 M KOH with a scan rate of 10 mV s^{-1} and a rotation speed of 1600 rpm.

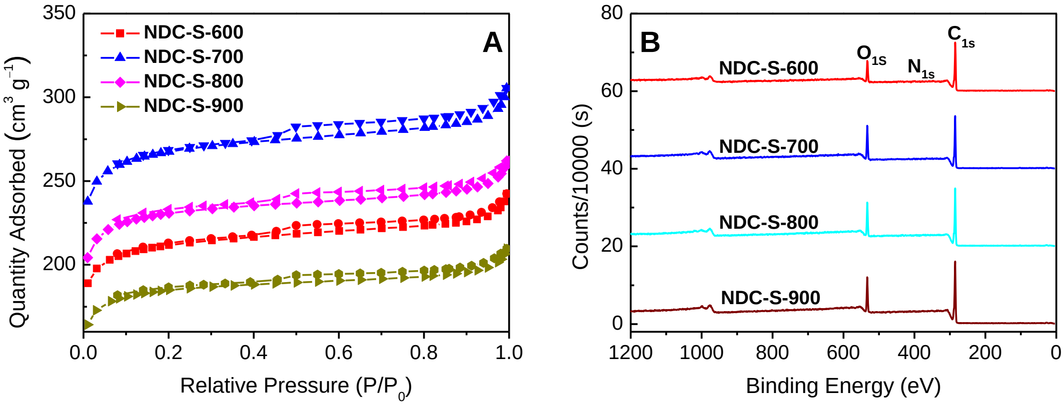

Fig. S14 A) N_2 adsorption–desorption isotherms and B) Full-scan XPS of NDC-S-600, NDC-S-700, NDC-S-800, NDC-S-900.

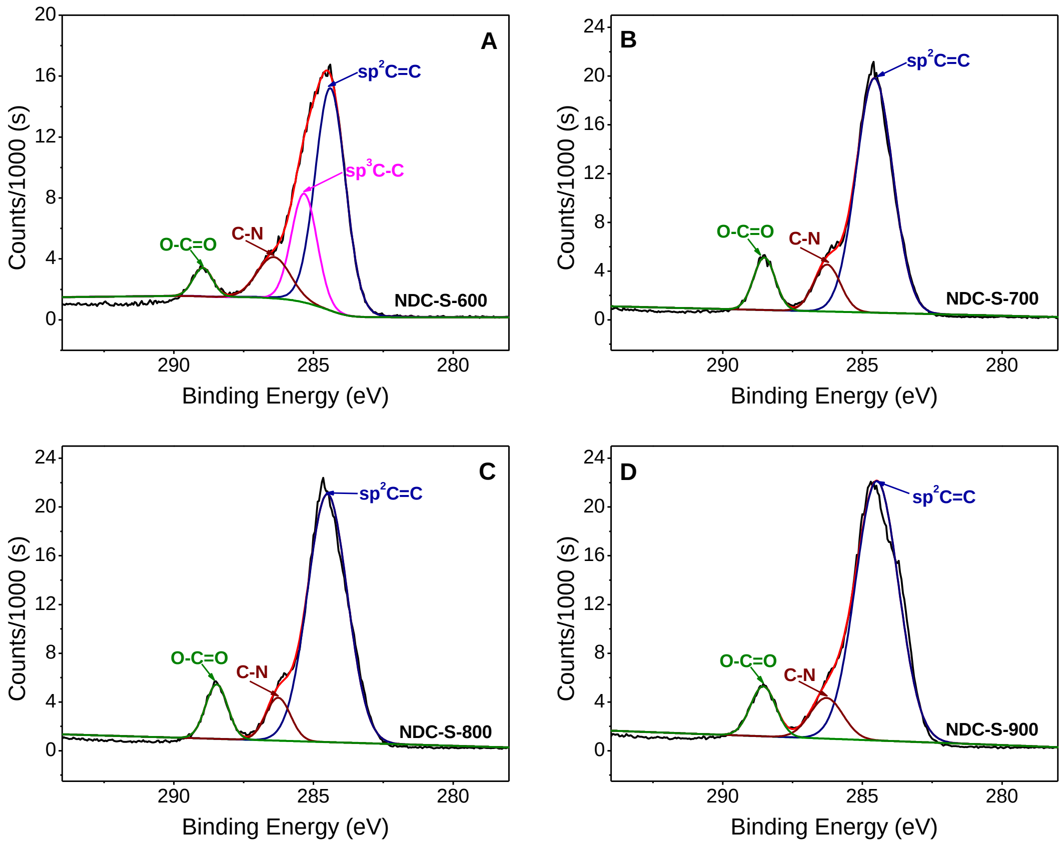

Fig. S15 C1s XPS spectra of NDC-S-600, NDC-S-700, NDC-S-800, NDC-S-900.

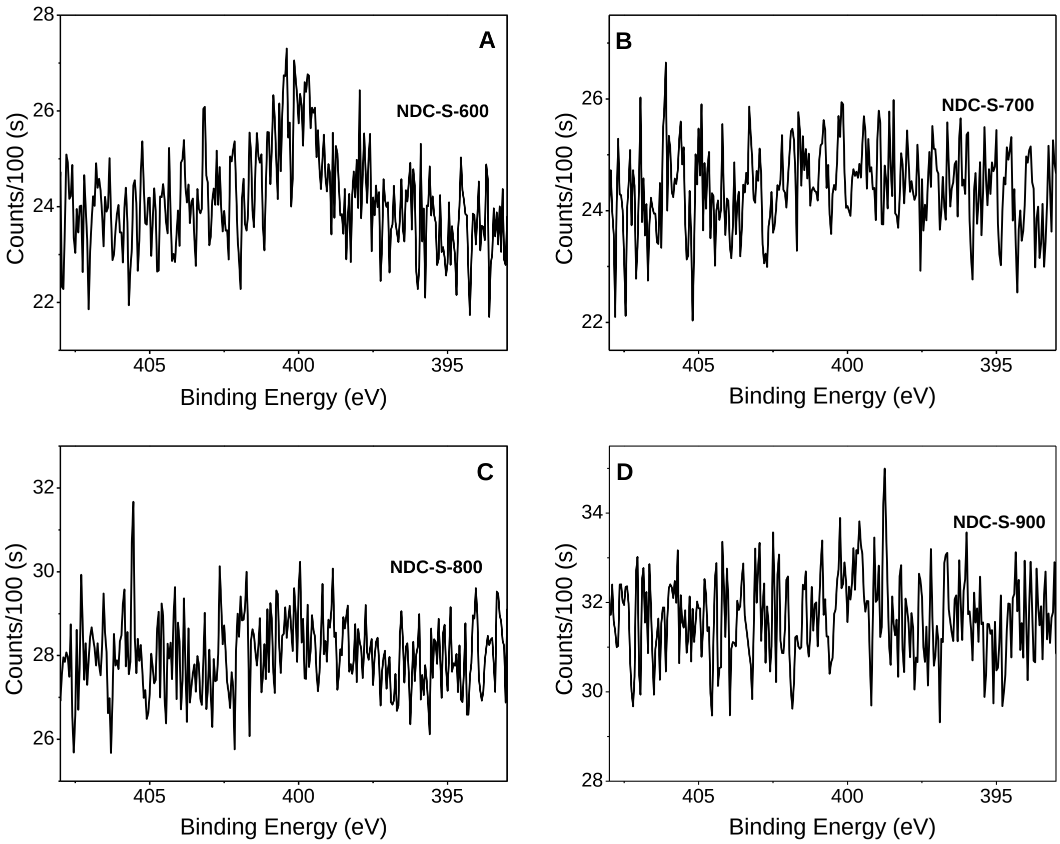

Fig. S16 High resolution N1s XPS scan of NDC-S-600, NDC-S-700, NDC-S-800, NDC-S-900.

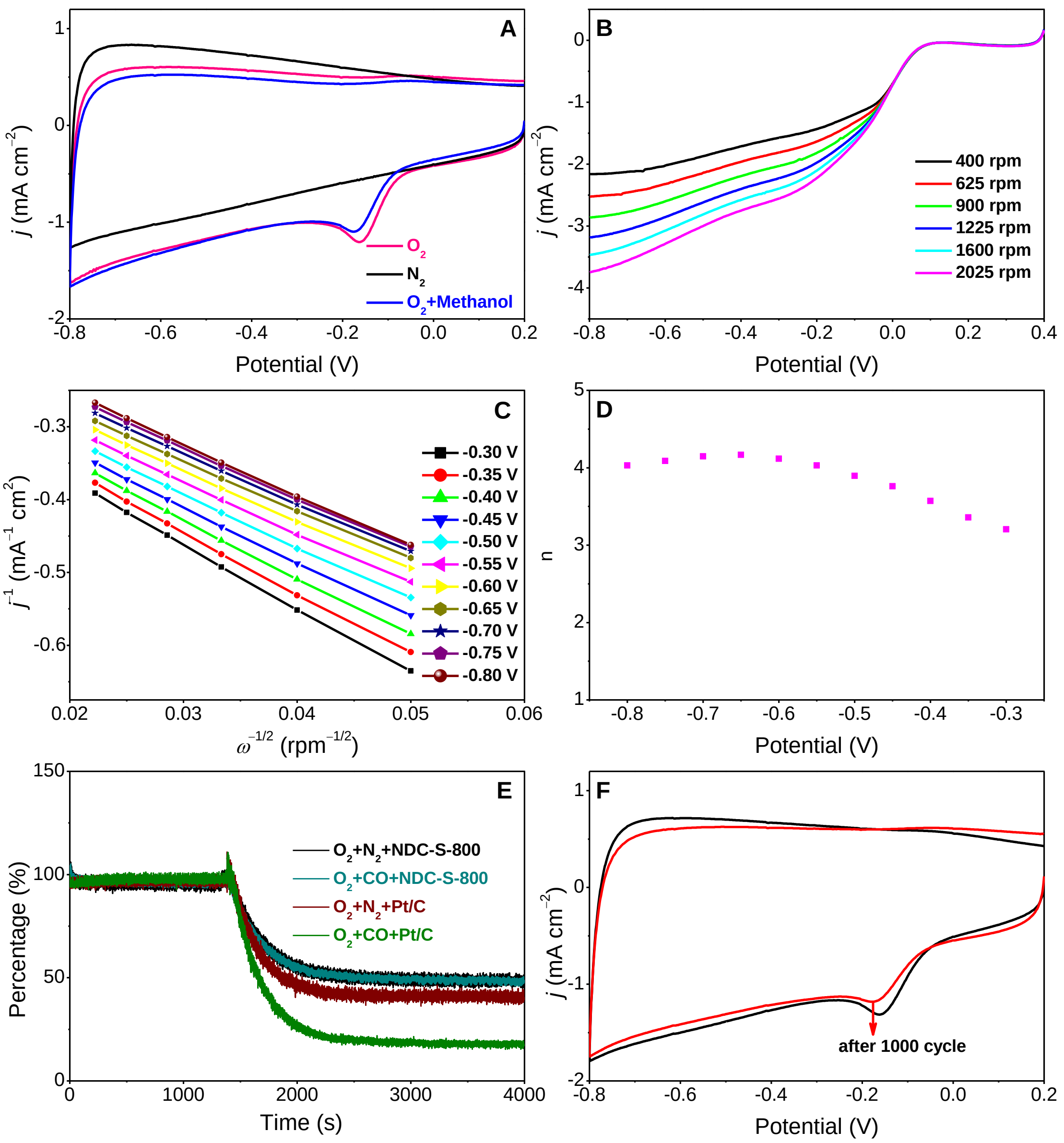

Fig. S17 A) CVs of NDC-S-800 in N_2-saturated, O_2-saturated 0.1 M KOH solution, and O_2-saturated 0.1 M KOH with 10 vol% methanol at a scan rate of 10 mV s^{-1}. B) RDE curves for NDC-S-800 in O_2-saturated 0.1 M KOH with a scan rate of 10 mV s^{-1} at different rotation speeds. C) K-L plots for the ORR in O_2-saturated 0.1 M KOH solution for NDC-S-800. D) The electron number calculated from K-L plot. E) The percentage of current density (j) vs. time chronoamperometric responses obtained at the NDC-S-800 and 20 wt% Pt/C electrodes at –0.30 V in O_2-saturated 0.1 M KOH. The arrow indicates the introduction of N_2 or CO into the electrolyte. F) Electrochemical stability of NDC-S-800 as determined by continuous CV scanning in O_2-saturated 0.1 M KOH. Scan rate: 10 mV s^{-1}.

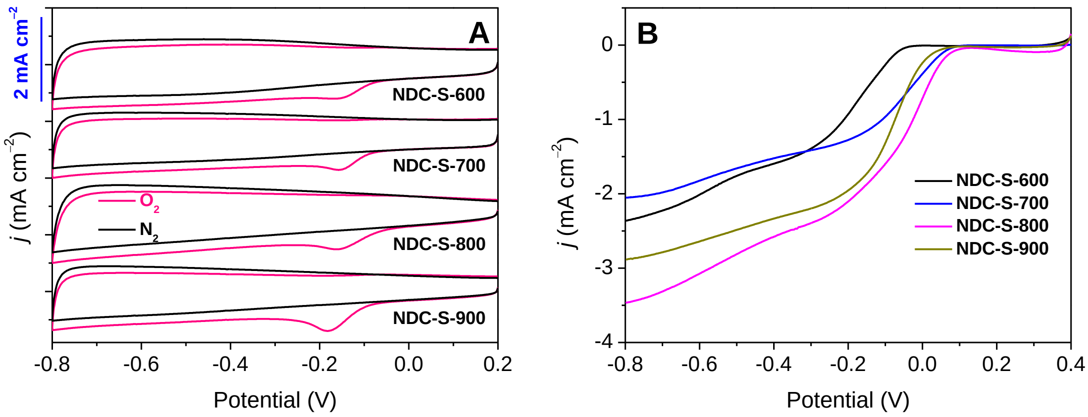

Fig. S18 A) CV curves of NDC-S-600, NDC-S-700, NDC-S-800, NDC-S-900 in N_2-saturated, O_2-saturated 0.1 M KOH solution at a scan rate of 10 mV s^{-1}. B) RDE curves for NDC-S-600, NDC-S-700, NDC-S-800, NDC-S-900 in O_2-saturated 0.1 M KOH with a scan rate of 10 mV s^{-1} and a rotation speed of 1600 rpm.

Table S1. Comparison of experimental conditions and ORR activities and kinetics of heteroatom-doped nanocarbon catalysts.

Catalyst	**Electrolyte**	**Reference electrode [a]**	**Half wave Potential (V vs RHE) [b]**	**Kinetic current at 0.8 V vs RHE (mA cm^{-2}) [c]**	**Reference**
CY-NDC	**0.1 M KOH**	**Hg/HgO**	**1.01**	**3.84 (@ 0.7 V)**	**This study**
N-CNT	0.1 M KOH	Ag/AgCl	0.81(CV) 0.75(LSV)	N/A	[1]
N-CNT	0.1 M KOH	Ag/AgCl	0.75	1.8	[2]
Polyelectrolyte-CNT	0.1 M KOH	SCE	0.68	0.33	[3]
B-CNT	1.0 M NaOH	SCE	0.6	0.70 (@ 0.7 V)	[4]
N-CNT	0.1 M KOH	Ag/AgCl	0.69 (CV)	N/A	[5]
N-CNT	0.1 M KOH	Hg/HgO	0.62	0.35 (@ 0.7 V)	[6]
B , N-CNT	0.1 M KOH	SCE	0.74	1.1	[7]
P , N-CNT	0.1 M KOH	SCE	0.75	3.0	[8]
B , N-CNT	1.0 M NaOH [d]	SCE	0.65	0.21	[9]
N-Graphene	0.1 M KOH	Ag/AgCl	0.62	0.12 (@ 0.7 V)	[10]
Polyelectrolyte-CNT	0.1 M KOH	SCE	0.60	0.83	[11]
N-CSs-800	0.1 M KOH	Hg/HgO	0.76	2.86 (@ 0.7 V)	[12]
S-Graphene	0.1 M KOH	Ag/AgCl	0.68	1.0	[13]
I-Graphene	0.1 M KOH	Ag/AgCl	0.68	0.71	[14]
N-Graphene	0.1 M KOH	Ag/AgCl	0.66	0.18	[15]
B-Graphene	0.1 M KOH	Ag/AgCl	0.51	0.85 (@ 0.7 V)	[16]
P-Graphite	0.1 M KOH	Ag/AgCl	0.56	0.83 (@ 0.7 V)	[17]
N , S-Graphene	0.1 M KOH	Ag/AgCl	0.59	0.40	[18]
B , N-Graphene	0.1 M KOH	Ag/AgCl	0.65	0.26	[19]
S1-AZ-800	0.1 M KOH	Hg/HgO	0.73	3.13 (@ 0.7 V)	[20]
N-OMC	0.1 M KOH	Ag/AgCl	0.62	2.2 (@ 0.7 V)	[21]
P-OMC	0.1 M KOH	Ag/AgCl	0.70	0.21	[22]
C_3N_4@OMC	0.1 M KOH	Ag/AgCl	0.67	2.1	[23]
N , O-OMC	0.1 M KOH	RHE	0.68	0.48	[24]
B-OMC	0.1 M KOH	Ag/AgCl	0.60	0.82 (@ 0.7 V)	[25]
Macroporous C_3N_4@Carbon	0.1 M KOH	Ag/AgCl	0.62	1.3 (@ 0.7 V)	[26]
Mesoporous N-Carbon	0.1 M KOH	Ag/AgCl	0.79	5.4	[27]
N-Carbon Nanocage	0.1 M KOH	Ag/AgCl	0.65	1.6 (@ 0.7 V)	[28]
N-Hollow Carbon NP	0.1 M KOH	Ag/AgCl	0.67	0.05	[29]
N-CDs	0.1 M KOH	Hg/HgO	0.63	3.92 (@ 0.7 V)	[30]

[a)] Conversions of Hg/HgO electrode, Ag/AgCl electrode, and SCE into RHE scale were achieved by adopting the calibration results; [b)]Half-wave potential was obtained from linear sweep voltammetry unless otherwise noted; [c)]Kinetic current at 0.8 V (vs RHE) was calculated by correction of diffusion-limited current. In some cases where kinetic current density was immeasurable at 0.8 V, the values at 0.7 V were used. [d)]RHE conversion in 1.0 M NaOH was estimated according to the Nernst equation. E(RHE) = E(SCE) + 59 mV = 1.045 V (59 mV per unit pH).

[S1]K. Gong, F. Du, Z. Xia, M. Durstock, L. Dai, *Science* **2009**, *323*, 760-764.

[S2]Z. Chen, D. Higgins, H. Tao, R. S. Hsu, Z. Chen, *J. Phys. Chem. C* **2009**, *113*, 21008-21013.

[S3]S. Wang, D. Yu, L. Dai, *J. Am. Chem. Soc.* **2011**, *133*, 5182-5185.

[S4]L. Yang, S. Jiang, Y. Zhao, L. Zhu, S. Chen, X. Wang, Q. Wu, J. Ma, Y. Ma, Z. Hu, *Angew. Chem. Int. Ed.* **2011**, *50*, 7132-7135.

[S5]Z. Wang, R. Jia, J. Zheng, J. Zhao, L. Li, J. Song, Z. Zhu, *ACS Nano* **2011**, *5*, 1677-1684.

[S6]T. Sharifi, G. Hu, X. Jia, T. Wågberg, *ACS Nano* **2012**, *6*, 8904-8912.

[S7]S. Wang, E. Iyyamperumal, A. Roy, Y. Xue, D. Yu, L. Dai, *Angew. Chem. Int. Ed.* **2011**, *50*, 11756-11760.

[S8]D. Yu, Y. Xue, L. Dai, *J. Phys. Chem. Lett.* **2012**, *3*, 2863-2870.

[S9]Y. Zhao, L. Yang, S. Chen, X. Wang, Y. Ma, Q. Wu, Y. Jiang, W. Qian, Z. Hu, *J. Am. Chem. Soc.* **2013**, *135*, 1201-1204.

[S10] L. Qu, Y. Liu, J.-B. Baek, L. Dai, *ACS Nano* **2010**, *4*, 1321-1326.

[S11] S. Wang, D. Yu, L. Dai, D. W. Chang, J.-B. Baek, *ACS Nano* **2011**, *5*, 6202-6209.

[S12] S. Y. Gao, Y. L. Chen, H. Fan, X. J. Wei, C. G. Hu, H. X. Luo, L. T. Qu, *J. Mater. Chem. A* **2014**, *2*, 3317-3324.

[S13] Z. Yang, Z. Yao, G. Li, G. Fang, H. Nie, Z. Liu, X. Zhou, X. Chen, S. Huang, *ACS Nano* **2012**, *6*, 205-211.

[S14] Z. Yao, H. Nie, Z. Yang, X. Zhou, Z. Liu, S. Huang, *Chem. Commun.* **2012**, *48*, 1027-1029.

[S15] S. Yang, X. Feng, X. Wang, K. Müllen, *Angew. Chem. Int. Ed.* **2011**, *50*, 5339-5343.

[S16] Z.-H. Sheng, H.-L. Gao, W.-J. Bao, F.-B. Wang, X.-H. Xia, *J. Mater. Chem.* **2012**, *22*, 390-395.

[S17] Z.-W. Liu, F. Peng, H.-J. Wang, H. Yu, W.-X. Zheng, J. Yang, *Angew. Chem. Int. Ed.* **2011**, *50*, 3237-3261.

[S18] J. Liang, Y. Jiao, M. Jaroniec, S. Z. Qiao, *Angew. Chem. Int. Ed.* **2012**, *51*, 11496-11500.

[S19] Y. Zheng, Y. Jiao, L. Ge, M. Jaroniec, S. Z. Qiao, *Angew. Chem. Int. Ed.* **2013**, *52*, 3110-3116.

[S20] S. Y. Gao, H. Fan, Y. L. Chen, L. Li, Y. Bando, D. Golberg, *Nano Energy* **2013**. *2*, 1261-1270.

[S21] R. Liu, D. Wu, X. Feng, K. Müllen, *Angew. Chem. Int. Ed.* **2010**, *49*, 2565-2569.

[S22] D. -S. Yang, D. Bhattacharjya, S. Inamdar, J. Park, J.-S. Yu, *J. Am. Chem. Soc.* **2012**, *134*, 16127-16130.

[S23] Y. Zheng, Y. Jiao, J. Chen, J. Liu, J. Liang, A. Du, W. Zhang, Z. Zhu, S. C. Smith, M. Jaroniec, G. Q. Lu, S. Z. Qiao, *J. Am. Chem. Soc.* **2011**, *133*, 20116-20119.

[S24] R. Silva, D. Voiry, M. Chhowalla, T. Asefa, *J. Am. Chem. Soc.* **2013**, *135*, 7823-7826.

[S25] X. Bo, L. Guo, *Phys. Chem. Chem. Phys.* **2013**, *15*, 2459-2465.

[S26] J. Liang, Y. Zheng, J. Chen, J. Liu, D. Hulicova-Jurcakova, M. Jaroniec, S. Z. Qiao, *Angew. Chem. Int. Ed.* **2012**, *51*, 3892-3896.

[S27] W. Yang, T. -P. Fellinger, M. Antonietti, *J. Am. Chem. Soc.* **2011**, *133*, 206-209.

[S28] S. Chen, J. Bi, Y. Zhao, L. Yang, C. Zhang, Y. Ma, Q. Wu, X. Wang, Z. Hu, *Adv. Mater.* **2012**, *24*, 5593-5597.

[S29] G. Ma, R. Jia, J. Zhao, Z. Wang, C. Song, S. Jia, Z. Zhu, *J. Phys. Chem. C* **2011**, *115*, 25148-25154.

[S30] S. Y. Gao, Y. L. Chen, H. Fan, X. J. Wei, C. G. Hu, L. X. Wang, L. T. Qu, *J. Mater. Chem. A* **2014**, *2*, 6320-6325.